ISSN 1027-5495. Functional Materials, 28, No.3 (2021), p. 505-511.
doi:https://doi.org/10.15407/fm28.03.505

Study on the microstructure and enhanced photocatalytic performance of $BiOCl_xBr_{1-x}$ solid solution

***Wei He*[1,2], *Gang Liao*[1,2]**

[1]Department of Traffic and Municipal Engineering, Sichuan College of Architectural Technology, 610399 Sichuan Chengdu, China
[2]Deyang Key Laboratory of Building and Bridge Structure Engineering, Sichuan College of Architectural Technology, 618000 Sichuan Deyang, China

Received June 25, 2021

The solid solution $BiOCl_xBr_{1-x}$ with different Br/Cl ratios was prepared by a simple low-temperature wet chemical method. The crystal structure, morphology and optical properties were characterized using X-ray diffraction, scanning electron microscopy with energy dispersive spectroscopy and diffuse reflectance spectra in the UV–visible region. RhB was chosen as the target pollutant; its degradation under light with a wavelength of > 400 nm was carried out to assess the photocatalytic efficiency of pre-prepared photocatalysts. The results showed that the microstructure and photocatalytic activity of the $BiOBr_xCl_{1-x}$ solid solution can be controlled by changing the Br/Cl ratio, the most optimal value of the Br/Cl ratio was 0.8:0.2. The reaction rate constant was 0.06446, which is 1.1 times higher than for pure BiOBr. This enhanced effect can be explained by the unique crystal structure and well-positioned macropores, which can reduce the band gap and facilitate the migration of RhB molecules. Our results can help to improve the photocatalytic performance of BiOX (X = Cl, Br and I).

Keywords: BiOX, solid solution, photocatalytic efficiency, wet chemical method.

Дослідження мікроструктури та поліпшених фотокаталітичних показників твердого розчину $BiOCl_xBr_{1-x}$. *Wei He, Gang Liao*

Твердий розчин $BiOCl_xBr_{1-x}$ з різним співвідношенням Br/Cl одержано простим методом низькотемпературної вологої хімії. Кристалічну структуру, морфологію і оптичні властивості охарактеризовано за допомогою рентгенівської дифракції, скануючої електронної мікроскопії з енерго-дисперсійною спектроскопією і спектрів дифузного відбиття в УФ–видимій області. В якості цільового забруднювача обрано RhB, його розкладання під світлом з довжиною хвилі > 400 нм проведено для оцінки фотокаталітичної ефективності заздалегідь приготованих фотокаталізаторів. Результати показали, що мікроструктуру і фотокаталітичну активність твердого розчину $BiOBr_xCl_{1-x}$ можна регулювати, змінюючи співвідношення Br/Cl, найбільш оптимальне значення відношення Br/Cl становило 0,8:0,2. Константа швидкості реакції становила 0,06446, що в 1,1 рази вище, ніж у чистого BiOBr. Цей посилений ефект можна пояснити унікальною кристалічною структурою і правильно розташованими макропорами, які можуть зменшити ширину забороненої зони і сприяти міграції молекул RhB. Наші результати можуть сприяти поліпшенню фотокаталітичних характеристик BiOX (X = Cl, Br і I).

Твердый раствор $BiOCl_xBr_{1-x}$ с различным соотношением Br/Cl приготовлен простым методом низкотемпературной мокрой химии. Кристаллическая структура, морфология и оптические свойства охарактеризованы с помощью метода рентгеновской дифракции,

сканирующей электронной микроскопии с энерго-дисперсионной спектроскопией и спектров диффузного отражения в УФ–видимой области. В качестве примеси выбран RhB, его разложение под светом с длиной волны > 400 нм проведено для оценки фотокаталитической эффективности предварительно приготовленных фотокатализаторов. Результаты показали, что микроструктуру и фотокаталитическую активность твердого раствора $BiOBr_xCl_{1-x}$ можно регулировать, изменяя соотношение Br/Cl, наиболее оптимальное значение отношения Br/Cl составляло 0,8:0,2. Константа скорости реакции составляла 0,06446, что в 1,1 раза выше, чем для чистого BiOBr. Этот усиленный эффект можно объяснить уникальной кристаллической структурой и правильно расположенными макропорами, которые могут уменьшить ширину запрещенной зоны и способствовать миграции молекул RhB. Наши результаты могут способствовать улучшению фотокаталитических характеристик BiOX (X = Cl, Br и I).

1. Introduction

In the 21st century, people are faced with a serious energy crisis and the problem of environmental pollution. Photocatalysis is of interest all over the world, because under the action of a photocatalyst, solar energy can be converted and stored in the form of chemical energy or used to eliminate environmental pollution [3, 4]. TiO_2 is the most widely used photocatalyst, but it can only be excited by UV light [1, 2]. Recently, scientists have been trying to discover new photocatalysts that respond to visible light, among which BiOX (X = Cl, Br, I) has great prospects due to its high photocatalytic activity, low cost and simple manufacturing process. BiOX (X = Cl, Br, I) is a highly anisotropic semiconductor with a layered structure, and the X atom is bonded in $[Bi_2O_3]$ + interlayers by the van der Waals force, which is weak, and thus the structure is loose and easily amenable to processing, dissociate in the direction of the (001) plane.

Despite of the unique structure, practical photocatalytic performance of pristine BiOX(X = Cl, Br, I) is also limited by some common drawbacks, such as a narrow light absorption range and a high tendency to the hole-electron recombination [4]. Moreover, BiOCl does not react well to visible light and BiOI is not stable in the photocatalytic process. Up to date, many methods have been applied to improve the photocatalytic property of BiOX; the methods can be classified into three categories, namely, element doping, morphology regulation and heterojunction construction. In terms of photocatalytic activity and stability in visible light, the complex properties of BiOBr are the best among BiOX. Previous research has proved that BiOX is a semiconductor with an indirect band gap, that is, the conduction band of BiOX is mainly in Bi(6*p*) orbit and the valence band is a hybrid of O(2*p*) and X(*np*) (*n* = 3, 4 and 5) orbitals [3]. In theory, doping of various X element can form different band structure, thus adjusting the position of the BiOX valence band.

In this paper, a facile low-temperature wet chemical method was used to prepare $BiOCl_xBr_{1-x}$ solid solution with different Br/Cl ratios. X-ray diffraction (XRD), scanning electron microscopy with energy dispersion spectroscopy (SEM-EDS), diffuse reflectance spectra (DRS) in the UV – visible range were applied to characterize the microstructure of as-prepared photocatalysts; degradation of RhB under visible-light irradiation was used to evaluate the photocatalytic performance.

2. Experimental

2.1 Materials

All the chemical reagents were purchased from Shanghai Taitan Technology Co., Ltd. They were analytical reagents and without further purification.

2.2 Sample preparation

A certain amount of $Bi(NO_3)_3 \cdot 5H_2O$ was added into 25 ml ethylene glycol (EG), and the solution was put in a 45°C water bath and then ultrasonically treated for 1 h until the $Bi(NO_3)_3 \cdot 5H_2O$ was totally solved forming solution *A*. A corresponding amount of KX X = Cl, Br were dissolved in 20 ml deionized water and stirred for 30 min to form solution *B*. Afterwards, the solution *B* was added into solution *A* with continuous stirring at the rate of 1–2 drop/s, then the mixture was stirred for another 2 h. Then, the precipitate was centrifugated and washed by ethanol (1 time) and deionized water (2 times). Finally, the product was dried in an oven at 80°C for 12 h to obtain the $BiOCl_xBr_{1-x}$ solid solution. The proportions of the mixtures of prepared samples are shown in Table 1.

2.3 Characterization

X-ray diffraction was measured on an X-ray diffraction detector (Rigaku D/max2550, Japan) with a Cu–Kα source

Table 1. Mixture proportions of prepared samples

	$Bi(NO_3)_3{\cdot}5H_2O$, mol	ethylene glycol, ml	KBr, mol	KCl, mol	Deionized water, ml
BiOBr	0.1	25	0.1	–	20
$BiOCl_{0.8}Br_{0.2}$	0.1	25	0.02	0.08	20
$BiOCl_{0.5}Br_{0.5}$	0.1	25	0.05	0.05	20
$BiOCl_{0.2}Br_{0.8}$	0.1	25	0.08	0.02	20

operating at 40 kV and 100 mA. The patterns between the diffraction angles (2θ) from 10 deg to 80 deg were continuously recorded with a step of 0.02 deg. Micromorphology was observed by scanning electron microscope (Hitachi TM4000 Plus, Japan) and the element distribution on a micro-area was detected using an energy dispersion spectroscope (IXRF, America). The samples were observed in the backscattered electron mode. Diffusion reflection spectra in the UV–visible range were registered with powder sample from spectrophotometer (Hitachi U-4100, Japan). The spectra were collected at 200–800 nm referenced to $BaSO_4$.

2.4 Photocatalytic performance tests

Photocatalytic performance of the $BiOCl_xBr_{1-x}$ solid solution was evaluated by degradation of RhB under visible light irradiation of a 500 W Xenon lamp with a 400 nm cutoff filters. 0.05 g specimen and 50 ml RhB aqueous solution (10 mg/L) were added into a Petri dish with a diameter of 10 cm. Before switching on the light, the Petri dish was placed in a dark place with continuous stirring for 10 min, realizing the adsorption equilibrium of RhB on the tested sample. Then the photocatalytic reaction was triggered after turning the Xenon lamp on. During the whole process, 3 ml of the RhB solution was sampled from the Petri dish with an interval of 10 min. And then all the sampled RhB solutions were centrifugated in a high-speed centrifuge at a speed of 10000 RCF for 5 min, and the supernatant was used for measuring its absorbance at the wave of 554 nm by a UV-vis spectrophotometer (Meipuda UV1200, China). The degradation rate of RhB can be calculated by Eq. (1), and according the first-order reaction model, the corresponding kinetics constants can be acquired by a linearly fitting $-\ln(C_t/C_0)$ and t, and the slope was the kinetics constant.

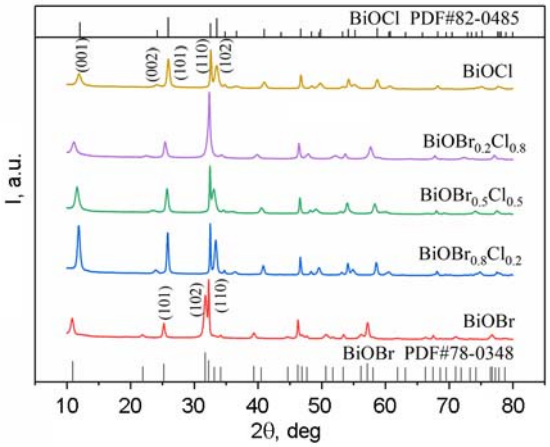

Fig. 1. X-ray diffraction patterns of specimens.

$$\delta = \frac{C_0 - C_t}{C_0} = \frac{A_0 - A_t}{A_0} \times 100\%, \qquad (1)$$

where C_0 is the initial concentration of RhB, C_t is the concentration of RhB at time t, A_0 is the initial absorbance, A_t is the absorbance at time t, and t is the reaction time.

3. Results and discussion

3.1 Microstructure analysis

Figure 1 displays the X-ray diffraction patterns of as-prepared samples. It can be clearly seen that the diffraction peaks of BiOBr sample matched well with those of a standard BiOBr pattern PDF#78-0348, demonstrating that the crystallization degree of fabricated BiOBr was relatively high and the reflections of crystal planes (101), (102), and (110) were observed. The same pattern was obtained for BiOCl in comparison with a standard BiOCl pattern PDF#82-0485. However, when Br and Cl were co-mixed, the X-ray diffraction patterns of the $BiOCl_xBr_{1-x}$ were different, depending on the Br/Cl ratio. Positions of most diffraction peaks were

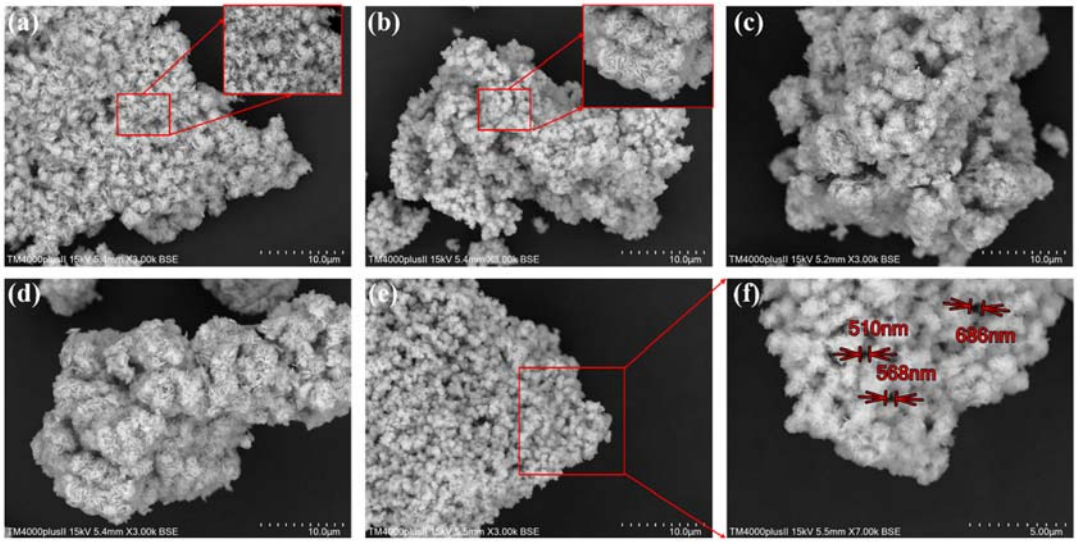

Fig. 2. SEM images of (a) BiOBr, (b) BiOCl, (c) $BiOCl_{0.8}Br_{0.2}$, (d) $BiOCl_{0.5}Br_{0.5}$, (e) $BiOCl_{0.2}Br_{0.8}$ and (f) $BiOCl_{0.2}Br_{0.8}$, ×7000 magnification.

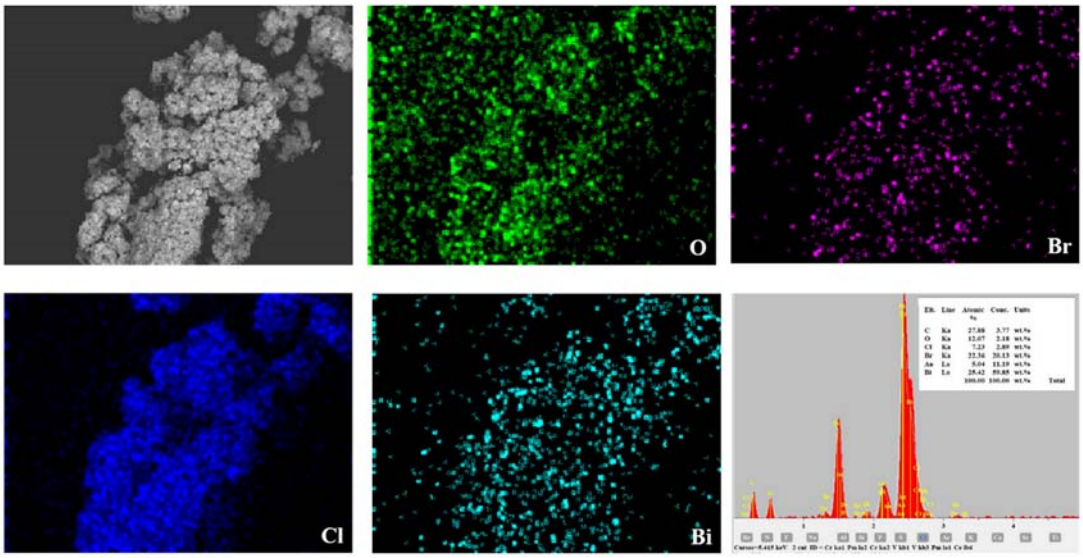

Fig. 3. Mapping of $BiOCl_{0.2}Br_{0.8}$ elements.

consistent with those of BiOBr, but some characteristic reflections changed, for instance, the (102) reflection disappeared in $BiOBr_{0.2}Cl_{0.8}$, while and its (110) reflection was intensified; the reflection (102) was observed for both $BiOCl_{0.2}Br_{0.8}$ and $BiOCl_{0.5}Br_{0.5}$. This can be explained by the fact that some crystal planes were distorted by co-doping of Br/Cl, due to their different extra-nuclear electron orbits, which may affect the band structure of BiOX, and this effect was related to the Br/Cl ratio.

Fig. 2 depicts the micro-morphology of as-prepared samples. As shown in Fig. 2a, BiOBr mainly consists of flower-like microspheres with a diameter of 1 μm that are self-assembled with nanosheets. From the magnified picture, this structure was found to be absolutely loose, favoring for the light transmitting and mass transfer. The images of rest samples are similar to those of BiOBr, and little difference can be found at such magnification (×3000). However, it should be noted that highly-aligned macropores (about 600 nm) were found in $BiOBr_{0.8}Cl_{0.2}$ as shown in Fig. 2f, which may affect its photodegradation performance. Fig. 3 presents the element mapping of $BiOCl_{0.2}Br_{0.8}$ sample; four elements, namely, Bi, O, Cl, and Br were detected. The distri-

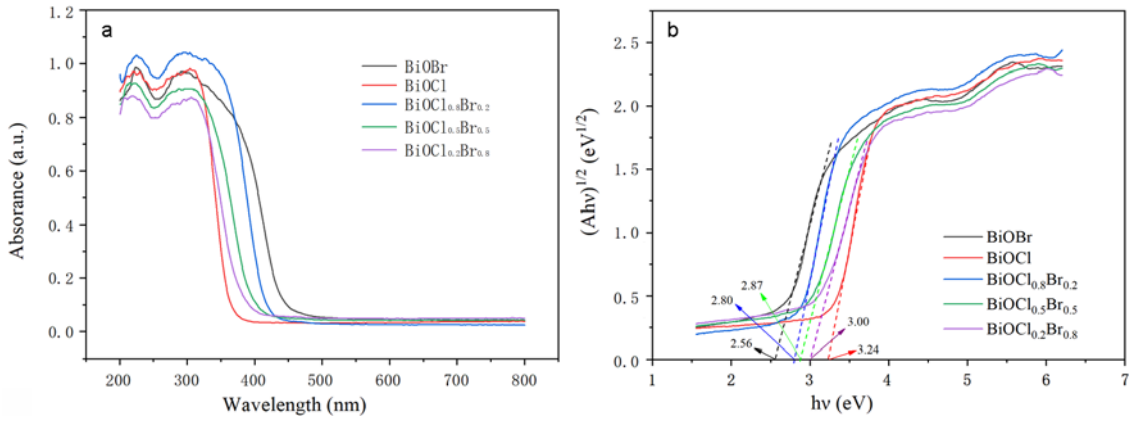

Fig.4. (a) UV-visible diffuse reflection spectra for all samples and (b) plots of (Ah)1/2 vs. h.

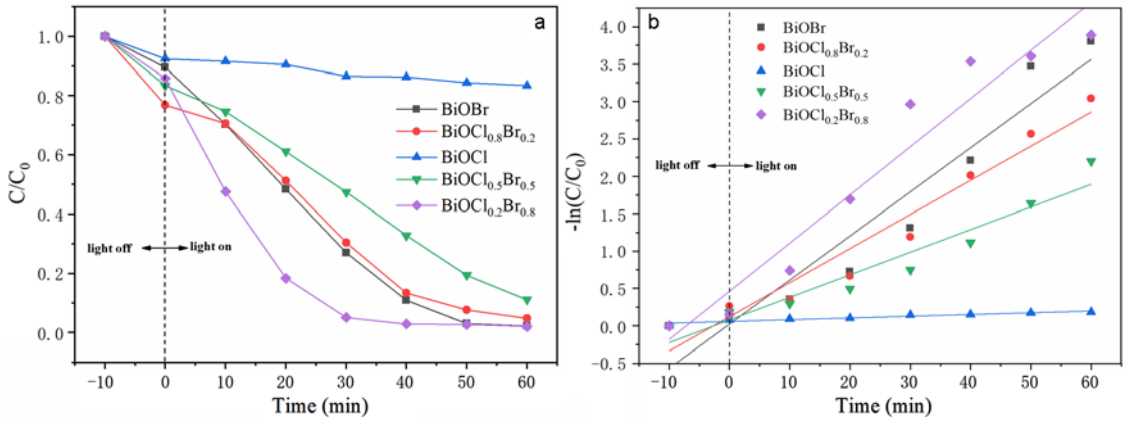

Fig. 5. (a) Variation of RhB concentration vs. time, (b) linear fitting curves of $-\ln(C_t/C_0)$ vs t.

bution of Cl and Br was almost duplicated with Bi, confirming the layered structure of BiOX. Cl and Br are distributed homogenously, which can guarantee the uniformity of the $BiOCl_{0.2}Br_{0.8}$; moreover, the atomic content of Br was 3 times higher than that of Cl, which corresponds to the calculated Br/Cl ratio.

Fig. 4 exhibits the optical property of $BiOCl_xBr_{1-x}$ samples. As shown in Fig. 4a, intensive absorption appeared at the range of 300–380 nm indicates that BiOCl can only be activated by UV-A. With increasing Br content, the absorption edge gradually shifts towards visible light, and the absorption edge of BiOBr can reach 460 nm. According to Tauc Plot, the band gap can be obtained from Fig. 4b, and the result shows that band gap decreases with increasing Br content, and BiOBr has the smallest band gap reaching 2.56 eV, which is consistent with the light absorption range.

3.2 Photocatalytic performance

Fig. 5 illustrates the efficiency of photocatalytic removal of RhB. As shown in Fig. 5a, before illumination, the concentration of the RhB solution decreased slightly due to physical adsorption of RhB in powder samples. After illumination, the RhB concentration immediately decreased, but the rate of decline varied depending on the Br/Cl ratio. BiOCl showed the slowest degradation rate of all samples, 12 % RhB degraded in just 60 minutes, suggesting that BiOCl has poor photocatalytic degradability in the visible region. The result is in accordance with the band gap of BiOCl, 3.24 eV, which can only be excited by light with the wavelength < 380 nm. The rest samples held the similar tendency, namely, RhB was continuously degraded under the illumination of visible light. However, the degradation rates were rather different; namely, $BiOCl_{0.2}Br_{0.8}$ had the highest degradation rate and almost all RhB was removed within only 30 min. The photocatalytic degradation ability of $BiOCl_{0.8}Br_{0.2}$ was equal to that of BiOBr, and

RhB could be completely removed with the two samples within 60 min. In the case of $BiOCl_{0.5}Br_{0.5}$, the degradation rate was lower than for BiOBr, with about 90 % RhB removal in 60 min. According to the first-order reaction model, the value $-\ln(C_t/C_0)$ linearly varies with the reaction time; and the slope represents the reaction rate constant k. The linear fitting curves are shown in Fig. 5b, the linear relationship between $-\ln(C_t/C_0)$ and t is obvious, indicating that the first-order reaction model can properly describe the photocatalytic reaction. The reaction rate constant and corresponding quality of fit are listed in Table 2. The quality of fit for all samples exceeds 90 %, which confirms the effectiveness of the first-order reaction model in interpreting the photocatalytic degradation of RhB. The reaction rate constant for BiOCl was only 0.00233 min^{-1}, which is much lower than for the rest of the samples. The reaction rate constant for $BiOBr_{0.8}Cl_{0.2}$ was the highest reaching 0.06446 min^{-1}, which is about 1.1 times higher than that of pure BiOBr; i.e. the photocatalytic efficiency of $BiOCl_{0.2}Br_{0.8}$ was 1.1 times higher. This is due to the unique crystal structure and porous morphology $BiOCl_{0.2}Br_{0.8}$ solid solution, as shown in XRD patterns and SEM images. For other $BiOBr_xCl_{1-x}$ solid solutions with various Br/Cl ratios, the rate constants were lower that of $BiOBr_{0.8}Cl_{0.2}$, suggesting that Br/Cl ratio of 0.8:0.2 was the critical value which resulted in the most optimal photocatalytic activity.

3.3 Possible mechanism

The photocatalytic degradation of RhB is a multi-steps process which is complex and can simply be divided into several steps. In the first step, physical adsorption dominates, and RhB molecules can freely move to the surface of $BiOBr_xCl_{1-x}$ under the effect of the Fick diffusion law. The RhB molecule size is about 1.59×1.18×0.56 nm, which is much smaller than the average pore diameter of $BiOBr_xCl_{1-x}$ solid solution; therefore, RhB molecules are easily captured by $BiOBr_xCl_{1-x}$until adsorption equilibrium is established. The result is that the concentration of RhB around the $BiOBr_xCl_{1-x}$ solid solution always remains at a high level. Once the $BiOBr_xCl_{1-x}$ is illuminated by visible light, electron-hole pairs would be generated on the surface of $BiOBr_xCl_{1-x}$, which would react with –OH and the dissolved O_2 in the aqueous solution, thus generating ROS such as hydroxide radicals and superoxide radicals in different chain reactions.

Table 2. Reaction rate constants and corresponding fitting goodness

	K/min^{-1}	R^2
BiOBr	0.05899	0.92451
$BiOBr_{0.2}Cl_{0.8}$	0.04563	0.9487
$BiOBr_{0.5}Cl_{0.5}$	0.03024	0.92984
$BiOBr_{0.8}Cl_{0.2}$	0.06446	0.94411
BiOCl	0.00233	0.90989

RhB would be mineralized into inorganic matters by these hydroxide radicals as shown in Eq. (2):

$$C_{28}H_{31}ClN_2O_3 + {-OH} \rightarrow CO_2 + H_2O. \quad (2)$$

When the captured RhB are consumed out by hydroxide radicals, the state of adsorption equilibrium is immediately disrupted, and more RhB molecules are adsorbed to the $BiOBr_xCl_{1-x}$ solid solution and then more RhB is decomposed again.

4. Conclusions

To summarize, we proposed a facile method to synthesize the $BiOBr_xCl_{1-x}$ solid solution. A number of $BiOBr_xCl_{1-x}$ solid solutions were prepared by changing the ratio of Br and Cl. In addition, the microstructure and photocatalytic activity of the $BiOBr_xCl_{1-x}$ solid solution can be regulated by changing Br/Cl ratio. The critical value of Br/Cl ratio was 0.8:0.2, which can provide the most optimal photocatalytic efficiency. Photocatalytic degradation of RhB indicated that $BiOCl_{0.2}Br_{0.8}$ displayed the highest photocatalytic activity, 1.1 times superior to that of pure BiOBr. This enhanced photocatalytic activity is due to the unique crystal structure and regularly-arranged macropores. The band gap was reduced noticeably by introducing Br. Our research may provide a simple but feasible method to modify BiOX(X = Cl, Br and I), realizing high photocatalytic efficiency.

Acknowledgement. This research was funded by Deyang Science and Technology Program (Nos. 2020SZZ047 and 2019SZ083).

References

1. S.K.Padmanabhan, S.Pal, E.Ul Haq et al., *Appl. Catal. A Gen.*, **485**, 157 (2014).
2. C.L.Bianchi, S.Gatto, C.Pirola et al., *Cem. Concr. Compos.*, **36**, 116 (2013).

3. A.Folli, C.Pade, T.B.Hansen et al., *Cem. Concr. Res.*, **42**, 539 (2012).
4. H.Jafari, S.Afshar, O.Zabihi et al., *Res. Chem. Intermed.*, **42**, 2963 (2016).
5. J.Yu, Y.Su, B.Cheng et al., *J. Mol. Catal. A: Chem.*, **258**, 104 (2006).
6. A.Fujishima, T.N.Rao, D.A.Tryk, *J. Photoch. Photobio. C.*, **1**, 1 (2000).
7. G.Cao, Z.Liu, *Mater. Lett.*, **202**, 32 (2017).
8. L.Lin, M.Huang, L.Long et al., *J. Alloys Compd.*, **615**, 929 (2014).
9. C.Xue, J.Xia, T.Wang et al., *Mater. Lett.*, **133**, 274 (2014).
10. Z.Jia, T.Li, Z.Zheng et al., *Chem. Eng. J.*, **380**, 122422 (2019).
11. B.Li, H.Huang, Y.Guo et al., *Appl. Surf. Sci.*, **353**, 1179 (2015).
12. Z.Liu, B.Wu, Y.Zhao et al., *Ceram. Int.*, **40**, 5597 (2014).
13. C.Xu, H.Wu, F.L.Gu, *J. Hazard. Mater.*, **275**, 185 (2014).
14. Y.Yang, C.Zhang, C.Lai et al., *Adv. Colloid Interface Sci.*, **254**, 76 (2018).
15. H.An, Y.Du, T.Wang et al., *Rare Metals*, **27**, 243 (2008).
16. Y.Wang, Q.Yang, X.Wang et al., *Mater. Sci. Eng. B-Adv.*, **244**, 12 (2019).